

# Potential Structure and Radial Profile of Neutron Production Rate in Spherical Inertial Electrostatic Confinement Plasmas

MATSUURA Hideaki\*, NAKAO Yasuyuki and KUDO Kazuhiko  
*Kyushu University, Hakozaki, Fukuoka 812-8581, Japan*

(Received: 5 December 2000 / Accepted: 27 August 2001)

## Abstract

The radial profile of neutron production rate in spherical inertial electrostatic confinement (SIEC) plasmas is investigated considering both of the beam (fuel ion)-beam and beam-target (background gas) fusion. The electrostatic potential is obtained by solving the Poisson equation, and by using the potential; fuel-ion velocity distribution function is determined at each radial point. From the velocity distribution function, the neutron production rate is evaluated. Numerical results show that although the total (volume-integrated) neutrons produced by beam-beam fusion are considerably lower than those of beam-target fusion, the effect of the beam-beam fusion on radial profile of the neutron production rate can be notable.

## Keywords:

IEC, ion distribution function, fusion reaction rate coefficient, neutron production rate

## 1. Introduction

The spherical inertial electrostatic confinement (SIEC) is a concept for electrostatically confining high-energy ions in potential well produced by circulating ions themselves [1-4]. In the spherical device, ions are accelerated toward the center of the sphere, and are again decelerated outward in the interelectrode space. In ideal SIEC plasmas, the ions converge toward the center of the device, and their space charge forms a virtual anode [5]. The cold electrons emitted from the cathode also converge toward the virtual anode, and are thought to create a virtual cathode inside area of the virtual anode. It is predicted that the multiple potential well hence appears, and fusion reaction is efficiently induced by accelerated fuel-ions trapped in the multiple well [1,4]. The multiple potential well is one of the key parameters for SIEC concept, and the appearance has been theoretically and experimentally investigated.

Fusion reactions in SIEC device were first realized by Hirsh [4] using high-energy ion guns as a source of

ions. He observed the double radial peak of the neutron production rate as well as the  $T(d,n)^4\text{He}(D(d,n)^3\text{He})$  neutron generation rate more than  $10^9$  ( $10^6$ ) n/s. The similar results, i.e. both double radial peak in neutron production rate and degree of the neutron production rate, were ascertained by Miley et al. [6]. They explained the current, pressure and external voltage dependence of neutron production rate by assuming that the fusion reactions occur between accelerated ions and background gas. The assumption that the neutron production is sustained mainly by the beam-target fusion implies that the effect of the double potential well formation on SIEC fusion is weak. It should be clarified why the double peak in radial profile of neutron production rate appears in such a state. Recently we showed the mechanism for double neutron peak can appear when neutrons are produced by the beam-target fusion without deep double potential well [7].

Thorson et al. [5] carried out the experiment to

\*Corresponding author's e-mail: [mat@nucl.kyushu-u.ac.jp](mailto:mat@nucl.kyushu-u.ac.jp)

examine the existence of the virtual cathode at the center of the sphere by directly measuring the potential using emissive probes. In their experiment virtual anode was observed in the converged core region, while no virtual cathode could be seen. In recent experiments by Yoshikawa *et al.* [8], in which he estimated the potential by means of the laser-induced fluorescence (LIF) method, the appearance of the double potential well was recognized. When the double potential well is formed, the radial profile of the neutron production rate may be more sensitively influenced, and then the effect of the beam-beam fusion would be more important.

In this paper, we consider a deuterium plasma confined in SIEC. In addition to the beam-target fusion, we newly include the effect of the beam-beam fusion and investigate the effect of the beam-beam fusion on radial profile of the neutron production rate.

## 2. Analysis Model

The SIEC is a weak collisional system, where the collision frequency and the fusion reaction rate are low compared with transit frequency of charged particles in a given electrostatic potential field. The motion of a charged particle in such a system is described by two constants of motion: the total energy  $E = 1/2mv^2 + q\phi$  and the angular momentum  $L = mrv_{\perp}$ . Here  $v_{\perp}$  represents the vertical velocity component, i.e.  $v_{\perp} = \sqrt{v_{\theta}^2 + v_{\phi}^2}$ , of a particle that has a velocity  $\mathbf{v} = (v_{\parallel}, v_{\theta}, v_{\phi})$  in spherical co-ordinates ( $v_{\parallel}$  is a radial velocity component). In this note, we assume that the deuteron is confined keeping the quantities  $E$  and  $L$  almost constant [9] and assume the distributions, using the dimensionless parameters  $\alpha$ ,  $\beta_a$  and  $\xi$ , in the following form [7]:

$$f_a(E, L) = c_a \exp \left[ - \left( \frac{E - |q_a \phi_0|}{\alpha E_0} \right)^2 - \left( \frac{L - \xi L_0}{B_a L_0} \right)^2 \right], \quad (1)$$

where subscript  $a$  represents particle species, i.e. deuteron or electron, grid voltage  $\phi_0$ ,  $E_0 = 10\text{keV}$  and  $L_0 = r_{\text{cat}} \sqrt{2m_D E_0}$ . Here  $r_{\text{cat}}$  is the radius of the spherical cathode. By adjusting  $\alpha$ ,  $\beta_a$  and  $\xi$  values, we can simulate the broadness of distributions toward energy and angular momentum. The coefficient  $c_a$  is determined so that the deuteron (electron) density at the cathode  $n_i(r_{\text{cat}})(n_e(r_{\text{cat}}))$  is equal to  $n_i^{\text{cat}}(n_e^{\text{cat}})$ . In this note, following Thorson's treatment [5,10], we relate  $n_i^{\text{cat}}$  to the measured cathode current  $I_{\text{meas}}$  by

$$n_i^{\text{cat}} = \frac{1}{1 - \gamma^2} \frac{1}{1 + \delta} \frac{I_{\text{meas}}}{4\pi r_{\text{cat}}^2 \sqrt{2e \phi_e / m_e}}, \quad (2)$$

where  $\gamma$  represents the transparency factor of inner grid [4] and  $\delta$  is the number of secondary electrons emitted from the grid due to ion impact [5]. Throughout the calculation,  $\gamma = 0.95$  [4] and  $\delta = 1$  [5] are assumed. We consider the secondary electrons emitted from the cathode with kinetic energy,  $\phi_e = 5\text{eV}$ . These electrons would pass through the core region only once, thus  $n_e^{\text{cat}}$  is related to the measured cathode current  $I_{\text{meas}}$  by

$$n_e^{\text{cat}} = \frac{\kappa}{1 + \delta} \frac{I_{\text{meas}}}{4\pi r_{\text{cat}}^2 \sqrt{2e \phi_e / m_e}}, \quad (3)$$

where roughly half of all the secondary electrons are assumed to be drawn inside the cathode, i.e. fraction of secondary electrons drawn inside the cathode is taken as  $\kappa = 0.5$ .

The electrostatic potential structure can be determined by Poisson's equation:

$$\nabla^2 \phi(r) = - \frac{q_i n_i(r) - q_e n_e(r)}{\epsilon_0}. \quad (4)$$

By integrating Eq.(1) using initial potential structure, we obtain the radial profile of deuteron and electron densities. By substituting the density profiles into Eq.(4), we solve Poisson's equation and get the potential structure again. This process is repeated until the calculation converges. From  $f_D(E, L)$  and  $\phi(r)$ , we can determine the space-dependent deuteron velocity distribution function  $f_D(r, v_{\parallel}, v_{\perp})$ , and using the velocity distribution function, the  $D(d,n)^3\text{He}$  fusion reaction rate coefficient is evaluated. From the reaction rate coefficient and deuteron and/or background deuterium densities, the radial profile of the neutron production rate owing to beam-beam or beam-target fusion can be estimated. Throughout the calculations, we assume that the background gas is confined uniformly in the spherical device. According to typical devices [2,6], the cathode radius is determined as  $r_{\text{cat}} = 3\text{cm}$ . The fusion cross sections are taken from the work of Duane [11] who assumed fusion reactions between bare nuclei.

## 3. Results and Discussion

In Fig.1 we first show the radial profiles of the electrostatic potential, deuteron and electron density, and beam-target  $D(d,n)^3\text{He}$  fusion reaction rate coefficient. In this calculation,  $\alpha = 0.04$ ,  $\beta_D = 0.20$ ,  $\beta_e = 0.0005$ ,  $\xi = 0.0$ , the grid voltage  $\phi_0 = 15\text{kV}$  and cathode current  $I_{\text{meas}} = 100\text{mA}$  are assumed. It is observed that

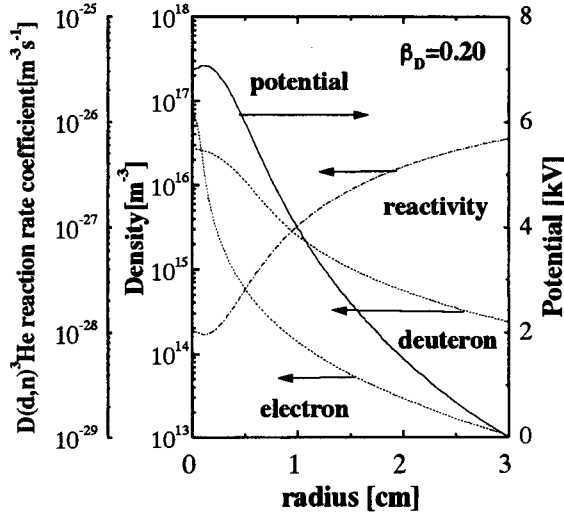


Fig. 1 Radial profile of deuteron and electron density, potential and beam-target  $D(d,n)^3\text{He}$  fusion reaction rate coefficient.

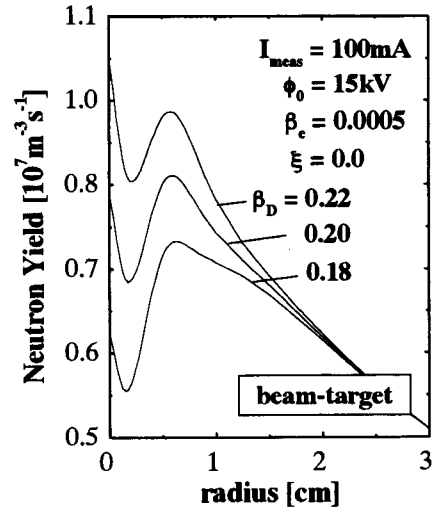


Fig. 2 Radial profile of  $D(d,n)^3\text{He}$  neutron production rate due to beam-target fusion.

both deuteron and electron densities increase with decreasing radius, together with the electrostatic potential. The ions slow down near the center core region due to the increased potential. Furthermore since the ion is assumed to move keeping its angular momentum almost constant, the velocity distribution function is close to isotropic form near the center core region [7]. (The vertical velocity component becomes larger as ion approaches the center of the sphere). The beam-target fusion reaction rate coefficient hence decreases with decreasing radius. Here the background deuterium gas is assumed to be Maxwellian of 0.1eV temperature and  $3 \times 10^{18} \text{m}^{-3}$  density.

By multiplying the beam-target fusion reaction rate coefficient by accelerated deuteron and background deuterium densities, the  $D(d,n)^3\text{He}$  neutron production rates are evaluated and the results are shown in Fig.2 for various  $\beta_D$  values. For small  $\beta_D$  values, the central peak of deuteron density becomes large, while the reaction rate coefficient more rapidly decreases with decreasing radius owing to the increment of the potential. Then neutron production rate has small values over entire radial range, and its radial peak moves outward from the center of the sphere. On the contrary, with increasing  $\beta_D$  values, the absolute values of the neutron production rate become large and the double peak begins to appear.

Now we examine the neutron production rate of beam-beam fusion. By multiplying the beam-beam fusion reaction rate coefficient by 1/2 and square of deuteron density at each radial point, i.e.  $(1/2)n_D^2$ , the

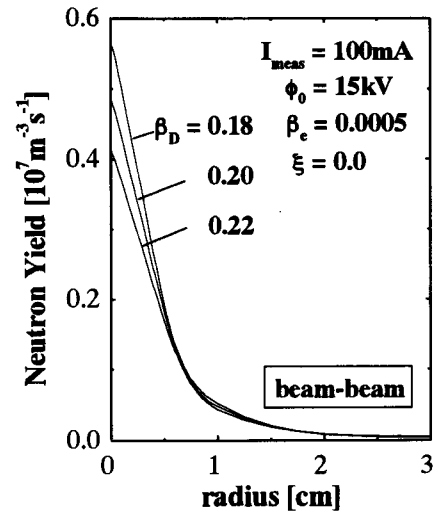


Fig. 3 Radial profile of  $D(d,n)^3\text{He}$  neutron production rate due to beam-beam fusion.

radial profile of the neutron production rate for beam-beam fusion is evaluated and the results are shown in Fig.3. The calculation parameters are same as those in Fig.2. It is observed the neutron production rate has a sharp peak at the center of the sphere. This is because the degree of the increase in square of deuteron density is larger than degree of the decrease in beam-beam fusion reaction rate coefficient over the entire radial range. The total neutron yield is calculated by integrating the neutron production rate inside the cathode, i.e.  $r \leq 3\text{cm}$ . For,  $\alpha = 0.04$ ,  $\beta_D = 0.20$ ,  $\beta_e =$

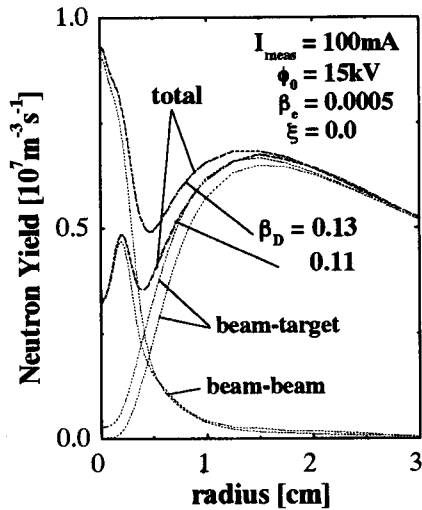


Fig. 4 Radial profile of  $D(d,n)^3\text{He}$  neutron production rate when both beam-target and beam-beam fusion is considered.

0.0005,  $\xi = 0.0$ , the grid voltage  $\phi_0 = 15\text{kV}$  and cathode current  $I_{\text{meas}} = 100\text{mA}$ , the neutron production rate due to beam-target fusion is  $6.6 \times 10^2 \text{n/s}$ , while the neutron production rate by beam-beam fusion is found to be  $1.5 \times 10^1 \text{n/s}$ . The effect of beam-beam fusion on radial profile of neutron production rate can be notable, although the total neutron yield due to beam-beam fusion is negligible compared with that due to beam-target fusion.

Next we examine the radial profile of the amount of the neutron production rate due to both beam-target and beam-beam fusion reactions. For  $\beta_D = 0.11$  and  $0.13$ , the radial profiles of the beam-target, beam-beam and total neutron production rates are exhibited in Fig.4. As was discussed in previous paragraph, for small  $\beta_D$  values, the neutron production rate by beam-target fusion becomes small especially in the center core region, owing to the reduction in fusion reaction rate coefficient by rapid increment of the potential. On the contrary, for beam-beam fusion, since the radial profile of the neutron production rate is influenced by density profile rather than reaction rate coefficient, a peak at the center of the sphere still remains. In Fig.4, the double

radial peak in total, i.e. beam-target plus beam-beam, neutron production rate thus appears.

To summarize, we have investigated the effect of the beam-beam fusion on radial profile of neutron production rate in SIEC plasmas. The effect of beam-beam fusion can be notable, although the total (volume-integrated) neutron yield due to beam-beam fusion is negligible compared with that due to beam-target fusion. It has also been shown that the double peak can appear in consequence of the combination of beam-target and beam-beam fusion neutrons. It should be noted that the amount of the beam-target fusion neutrons strongly depends on the background gas pressure, while the amount of the beam-beam fusion neutrons does not depend on the background gas pressure. The amount of the beam-beam neutrons is determined mainly by the plasma current. When the gas density is lower than  $\sim 10^{19} \text{m}^{-3}$  and plasma current is larger than  $\sim 100\text{mA}$ , the effect of the beam-beam fusion on radial profile of the neutron production rate begins to appear.

In this note, we have chosen the adequate  $\beta_D$  and  $\beta_e$  values to numerically reproduce the double peak in radial profile of the neutron production rate, and have shown a possible mechanism for the double peak appearance. In order to verify the mechanism, it would be necessary to identify the ion and electron distributions in experiments.

## References

- [1] W.C. Elmore *et al.*, Phys. Fluids **2**, 239 (1959).
- [2] G.H. Miley *et al.*, Fusion Eng. and Design **41**, 461 (1998).
- [3] M. Ohnishi *et al.*, Nucl. Fusion **37**, 611 (1997).
- [4] R.L. Hirsh, Phys. Fluids **11**, 2486 (1968).
- [5] T.A. Thorson *et al.*, Phys. Plasmas **4**, 4 (1997).
- [6] G.H. Miley *et al.*, Fusion Technol. **19**, 840 (1991).
- [7] H. Matsuura *et al.*, Nucl. Fusion **40**, 1951 (2000).
- [8] K. Yoshikawa *et al.*, Proc. of SOFE99, Albuquerque, 1999, IAE-RR-99 078 (1999).
- [9] W.M. Nevins, Phys. Plasmas **2**, 3804 (1995).
- [10] T.A. Thorson *et al.*, Nucl. Fusion **38**, 495 (1998).
- [11] B.H. Duane, BNWL-1685, Battelle Pacific Northwest Lab. (1972).